Attosecond pulses at kiloelectronvolt photon energies from high-order harmonic generation with core electrons

Christian Buth,[1,2,*] Feng He (何峰),[2,3,†] Joachim Ullrich,[2,4] Christoph H. Keitel,[2] and Karen Z. Hatsagortsyan[2]

[1] *Argonne National Laboratory, Argonne, Illinois 60439, USA*
[2] *Max-Planck-Institut für Kernphysik, Saupfercheckweg 1, 69117 Heidelberg, Germany*
[3] *Laboratory for Laser Plasmas and Department of Physics, Shanghai Jiao Tong University, Shanghai 200240, China*
[4] *Physikalisch-Technische Bundesanstalt, Bundesallee 100, 38116 Braunschweig, Germany*

(Dated: 05 March 2012)

High-order harmonic generation (HHG) in simultaneous intense near-infrared (NIR) laser light and brilliant x rays above an inner-shell absorption edge is examined. A tightly bound inner-shell electron is transferred into the continuum. Then, NIR light takes over and drives the liberated electron through the continuum until it eventually returns to the cation leading in some cases to recombination and emission of a high-harmonic photon that is upshifted by the x-ray photon energy. We develop a theory of this scenario and apply it to 1*s* electrons of neon atoms. The boosted high harmonic light is used to generate a single attosecond pulse in the kiloelectronvolt regime. Prospects for nonlinear x-ray physics and HHG-based spectroscopy involving core orbitals are discussed.

PACS numbers: 41.60.Cr, 32.80.Aa, 32.30.Rj, 42.65.Ky

High-order harmonic generation (HHG) by atoms in intense near-infrared (NIR) laser fields is a fascinating phenomenon and a versatile tool; it has spawned the field of attoscience, is used for spectroscopy, and serves as a light source in many optical laboratories [1–3]. Within the single-active electron (SAE) approximation [4–6] and the three-step model of HHG [7, 8], the NIR laser tunnel ionizes a valence electron and accelerates it in the continuum. When the NIR laser field changes direction, the liberated electron is driven back to rescatter with the parent ion. This may cause the electron to recombine with the ion whereby the excess energy due to the atomic potential and due to the energy gained from the NIR laser field is released in terms of a high harmonic (HH) of the NIR frequency. Frequently, this mindset is also applied to two-color HHG where a NIR laser is combined with VUV/XUV light [9, 10] which thereby assists in the ionization process leading to an overall increased yield [9, 11, 12]. This principle is evolved further by using attosecond XUV pulses to boost the HHG process which increases the yield for a certain frequency range by enhancing the contribution from specific quantum orbits [13–18]. However, there are only few exceptions, e.g., Refs. 19–22, in which many-electron effects are treated for two-color HHG. Fleischer [20] includes implicitly other electrons by using a frequency-dependent polarizability for the atoms. Then the XUV light is found to cause new plateaus to emerge at higher energies, however, with a much lower HH yield. Explicit two-electron effects in two-color HHG are considered in Refs. 21 and 22; there, the XUV photon energy is tuned to the core-valence resonance in the transient cation that is produced in the course of the HHG process by tunnel ionization. This leads to a second high-yield plateau that is shifted to higher energies by the XUV photon energy.

In this letter, we consider even higher photon energies where core electrons directly couple to the continuum using x rays from a free electron laser (FEL) such as the Linac Coherent Light Source (LCLS) [23, 24]. Our SAE scheme is depicted in Fig. 1 and proceeds in allusion to the three-step model of HHG [7, 8] as follows: (a) a core electron is ionized by one-x-ray-photon absorption; (b) the liberated electron propagates freely; (c) in some cases the electron is driven back to the ion and recombines with it emitting HH radiation. Although Fig. 1a suggest that the electron is born at a specific phase of the NIR light, this is not the case; instead, electrons are ejected during the entire x-ray pulse. This lifts restrictions of the width of the HHG plateau similarly to studies of HHG with valence-ionization by XUV light [16–18]. We exemplify our method for 1*s* electrons of neon with an ionization potential (IP) of $I_\mathrm{P} = 870.2\,\mathrm{eV}$ [25]. This yields boosted HH radiation at close to kiloelectronvolt photon energies from which we isolate a single attosecond pulse. All equations are formulated in atomic units.

Our scheme offers completely new prospects for HHG by involving core electrons. It thus goes beyond just an extension of the HHG cutoff into the kiloelectronvolt regime for which one may use conventional concepts that

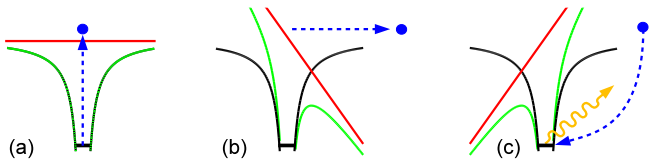

FIG. 1. (Color online) Schematic of the three-step model for the HHG process modified by x-ray induced ionization of a core electron. See text for details.

are laboratory size and valence-electron-based. Here it has been shown recently using midinfrared lasers [26] at high intensities of $\sim 10^{15}\,\mathrm{W/cm^2}$ that good HH yields can be obtained even in the presence of enhanced ionization by a judicious choice of the gas pressure [27–29].

In our quantum theory of x-ray ionization-based HHG, we make the SAE [4–6]. The ground state $|\,0\rangle$ is represented by the electron in the core orbital of the atomic ground state. Continuum states are described by plane waves $|\,\vec{k}\rangle$ for $\vec{k} \in \mathbb{R}^3$ where we neglect the impact of the atomic potential which is called the strong-field approximation. There are two processes which destroy the system and inhibit HHG. First, even in field-free conditions, core holes decay with a corresponding width Γ_c. Second, for two-color light additional valence-shell photoionization occurs for neutral and core-ionized neon induced by both, the NIR laser and the x rays [30]. The total destruction rates are expressed as $\Gamma_0(t)$ and $\Gamma_{\vec{k}}(t)$ for the neutral and the core-ionized states, respectively. They depend on time because the photoionization rate depends on the envelope of the NIR and x-ray pulse. Here "$\vec{k}$" is only a label as $\Gamma_{\vec{k}}(t)$ depends only negligibly on $\vec{k}$ for fast continuum electrons.

Based on the above model of an atom in two-color light, we derive equations of motion (EOMs) for its time evolution using the following ansatz for the SAE wavepacket

$$|\,\Psi, t\rangle = \mathrm{e}^{\mathrm{i}\,I_\mathrm{P}\,t}\,\Big[a(t)\,|\,0\rangle + \int\limits_{\mathbb{R}^3} b(\vec{k},t)\,|\,\vec{k}\rangle\;\mathrm{d}^3k\Big]\,, \qquad (1)$$

where I_P is the IP of the core electron. The Hamiltonian of the model is $\hat{H} = \hat{H}_\mathrm{A} + \hat{H}_\mathrm{L} + \hat{H}_\mathrm{X}$; it consists of the atomic electronic structure Hamiltonian $\hat{H}_\mathrm{A}$ and the coupling of the SAE to the NIR laser $\hat{H}_\mathrm{L}$ and the x rays $\hat{H}_\mathrm{X}$ in electric dipole approximation in length form [31]. Inserting Eq. (1) into the time dependent Schrödinger equation and projecting onto $\langle\,0\,|$ yields the EOM for the ground-state amplitude

$$\mathrm{i}\,\dot{a}(t) = -\frac{\mathrm{i}}{2}\Gamma_0(t)\,a(t) + E_\mathrm{X}(t)\int\limits_{\mathbb{R}^3} b(\vec{k},t)\,\langle\,0\,|\,\vec{e}_\mathrm{X}\cdot\vec{r}\,|\,\vec{k}\,\rangle\;\mathrm{d}^3k\,. \qquad (2)$$

Projecting onto $\langle\,\vec{k}\,|$ for all $\vec{k} \in \mathbb{R}^3$ results in EOMs for the continuum amplitude

$$\mathrm{i}\,\frac{\partial b(\vec{k},t)}{\partial t} = \Big[I_\mathrm{P} + \frac{\vec{k}^2}{2} - \frac{\mathrm{i}}{2}\,\Gamma_{\vec{k}}(t)\Big]\,b(\vec{k},t) + \mathrm{i}\,\vec{E}_\mathrm{L}(t)\cdot\vec{\nabla}_k\,b(\vec{k},t) + a(t)\,E_\mathrm{X}(t)\;\langle\,\vec{k}\,|\,\vec{e}_\mathrm{X}\cdot\vec{r}\,|\,0\,\rangle\;, \qquad (3)$$

where $\vec{r}$ is the electric dipole and $\vec{e}_\mathrm{X}$ is the linear polarization vector of the x rays. Inner-shell electrons are tightly bound such that the NIR laser hardly affects them. Hence, in the transition matrix elements only the x-ray term is relevant, i.e., $\langle\,\vec{k}\,|\,\hat{H}_\mathrm{X}\,|\,0\,\rangle$. Conversely, only the NIR laser impacts continuum electrons noticably, i.e., $\langle\,\vec{k}\,|\,\hat{H}_\mathrm{L}\,|\,\vec{k}'\,\rangle = \mathrm{i}\,\vec{\nabla}_k\,\delta^3(\vec{k}-\vec{k}')$.

To solve the coupled system of first-order partial differential equations (2) and (3), we realize that we may neglect the second term on the right-hand side of Eq. (2) [5]. This approximation decouples Eq. (2) from Eq. (3) which can now be integrated directly assuming that there is no light for $t < 0$. Then, the solution is unity for $t < 0$ and $a(t) = \mathrm{e}^{-\frac{1}{2}\Gamma_0(t)}$ for $t \geq 0$ where the temporal destruction exponent is defined by $\Gamma_i(t) = \int\limits_0^t \Gamma_i(t')\,\mathrm{d}t'$ for $i \in \{0\} \cup \{\vec{k} \mid \forall\,\vec{k} \in \mathbb{R}^3\}$. With the closed-form solution of Eq. (2), we can now integrate Eq. (3) formally exactly by introducing the canonical momentum $\vec{p} = \vec{k} - \vec{A}_\mathrm{L}(t)$ with the vector potential of the NIR laser $\vec{A}_\mathrm{L}(t)$ [5]. The saddle point approximation is used to simplify the triple integration over $\vec{p}$ in the calculation of the electric dipole transition matrix element $D(t) = \int\limits_{\mathbb{R}^3} a^*(t)\;\langle\,0\,|\,\vec{e}_\mathrm{D}\cdot\vec{r}\,|\,\vec{k}\,\rangle\;b(\vec{k},t)\;\mathrm{d}^3k = D'(t)\,\mathrm{e}^{-\mathrm{i}\,\omega_\mathrm{X}\,t}$ along the direction $\vec{e}_\mathrm{D}$ which determines the HH emission [5, 7, 8, 21, 22, 32] with the slowly varying dipole moment

$$\begin{aligned} D'(t) = -\frac{\mathrm{i}}{2}\int\limits_0^\infty \sqrt{\frac{(-2\,\pi\,\mathrm{i})^3}{\tau^3}}\;\langle\,0\,|\,\vec{e}_\mathrm{D}\cdot\vec{r}\,|\,\vec{p}_\mathrm{st}(t,\tau) + \vec{A}_\mathrm{L}(t)\,\rangle \\ \times\,\langle\,\vec{p}_\mathrm{st}(t,\tau) + \vec{A}_\mathrm{L}(t-\tau)\,|\,\vec{e}_\mathrm{X}\cdot\vec{r}\,|\,0\,\rangle\;\mathrm{e}^{-i\,S_\mathrm{st}(t,\tau)} \qquad (4) \\ \times\,\mathcal{E}_\mathrm{X}(t-\tau)\;\mathrm{e}^{-\frac{1}{2}\,[\Gamma_0(t)+\Gamma_0(t-\tau)+\Gamma_{\vec{k}}(t)-\Gamma_{\vec{k}}(t-\tau)]}\,\mathrm{d}\tau\,. \end{aligned}$$

We introduced the excursion time $\tau = t - t'$; at the stationary point (saddle point), the momentum is $\vec{p}_\mathrm{st}(t,\tau) = -\frac{1}{\tau}\int\limits_{t-\tau}^{t} \vec{A}_\mathrm{L}(t')\,\mathrm{d}t'$ and the quasiclassical action is

$$S_\mathrm{st}(t,\tau) = \int\limits_{t-\tau}^{t}\Big[\frac{1}{2}\,\big(\vec{p}_\mathrm{st}(t,\tau) - \vec{A}_\mathrm{L}(t')\big)^2 + I_\mathrm{P} - \omega_\mathrm{X}\Big]\,\mathrm{d}t'\,. \qquad (5)$$

Further, we employed the rotating-wave approximation [31] such that in Eq. (3) only the positive frequency components of the x-ray electric field $E_\mathrm{X}^+(t)$ are taken leading to the term involving "$-\omega_\mathrm{X}$" in Eq. (5) via the decomposition $E_\mathrm{X}^+(t) = \frac{1}{2}\,\mathcal{E}_\mathrm{X}(t)\,\mathrm{e}^{-\mathrm{i}\,\omega_\mathrm{X}\,t}$ with the complex field envelope $\mathcal{E}_\mathrm{X}(t) = E_{0\mathrm{X}}(t)\,\mathrm{e}^{-\mathrm{i}\,[\varphi_\mathrm{X}(t)+\varphi_{\mathrm{X},0}]}$, the real field envelope $E_{0\mathrm{X}}(t)$, the time-dependent phase $\varphi_\mathrm{X}(t)$, and the carrier to envelope phase (CEP) $\varphi_{\mathrm{X},0}$ [33].

The HHG spectrum follows from $D(t)$ by Fourier transformation. The transforms of $D(t)$ and $D'(t)$ are related by $\tilde{D}(\omega) = \tilde{D}'(\omega - \omega_\mathrm{X})$, i.e., the entire harmonic spectrum is shifted by ω_X toward higher energies. The harmonic photon number spectrum (HPNS) [21, 22, 32] of a single atom—i.e., the probability to find a photon with specified energy—along the propagation axis of the NIR laser is

$$\frac{\mathrm{d}^2P(\omega)}{\mathrm{d}\omega\,\mathrm{d}\Omega} = 4\,\pi\,\omega\,\varrho(\omega)\,|\tilde{D}(\omega)|^2\,, \qquad (6)$$

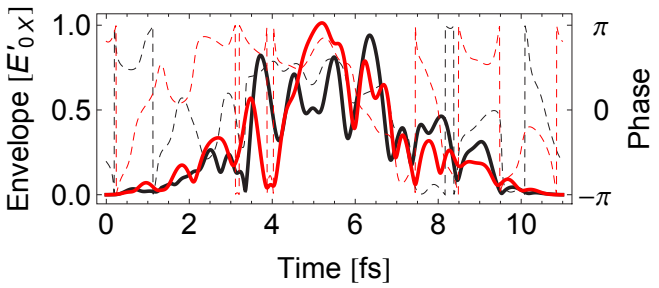

FIG. 2. (Color) Two exemplary SASE x-ray FEL pulses (black and red) for an x-ray photon energy of $\omega_{\rm X} = 569\,\omega_{\rm L} = 881.8\,{\rm eV}$. The envelope $E_{0{\rm X}}(t)$ is specified in units of the peak electric field $E'_{0{\rm X}}$ for the given peak x-ray intensity of $7.5 \times 10^{14}\,{\rm W/cm^2}$ and is represented by the solid lines whereas the phase $\varphi_{\rm X}(t)$ is depicted as dashed lines with CEP $\varphi_{{\rm X},0} = 0$. The average FWHM pulse duration is 1.5 optical cycles with a cosine square pulse envelope [34]. The average pulse spectrum is Gaussian and has a FWHM bandwidth of 8 eV which corresponds to a coherence time of 0.24 fs.

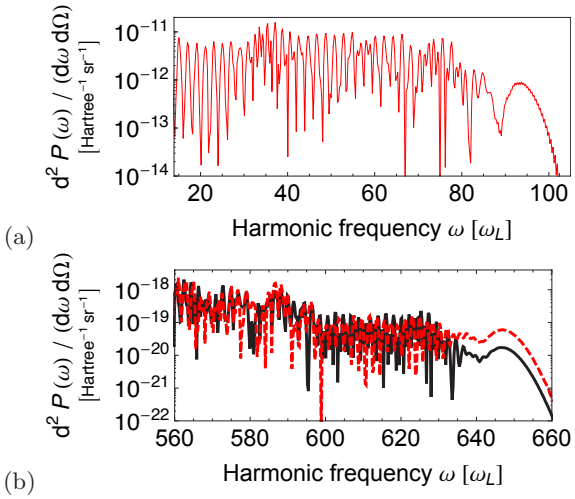

FIG. 3. (Color online) Harmonic photon number spectra (HPNS) [Eq. (6)] (a) for Ne $2p$ valence electrons and (b) for Ne $1s$ core electrons using the SASE pulses of Fig. 2. The solid, black line is from the black SASE pulse and the dashed, red line from the red pulse. The x-ray intensity [caption of Fig. 2] was chosen such that the ionization rate is the same as the tunnel ionization rate by the NIR laser. The NIR laser vector potential $A_{\rm L}(t)$ has a cosine square pulse envelope [34] with a FWHM duration of 1.5 optical cycles, CEP $\varphi_{{\rm L},0} = \pi/2$, and a peak intensity of $3 \times 10^{14}\,{\rm W/cm^2}$ for 800 nm central wavelength, i.e., the central photon energy is $\omega_{\rm L} = 1.55\,{\rm eV}$.

with the density of free-photon states $\varrho(\omega) = \frac{\omega^2}{(2\pi)^3\,c^3}$ [31], the speed of light in vacuum c, and the solid angle Ω.

We apply our theory to generate HH radiation from $1s$ core electrons of a neon atom where the polarization vectors of NIR laser $\vec{e}_{\rm L}$ and x rays $\vec{e}_{\rm X}$ and $\vec{e}_{\rm D}$ are along the z axis. To calculate the $1s$ orbital of neutral neon, we use the program of Herman and Skillman setting $\alpha = 1$ [35–37]. For the experimental core-hole width, $\Gamma_{\rm c} = 0.27\,{\rm eV}$, is used from Ref. 25. Present-day FELs generate x rays on the basis of the SASE principle [23, 24]. We model SASE pulses with the partial coherence method [38–40]. Two sample pulses are displayed in Fig. 2 where modeling parameters are specified in the figure caption. The chosen $\omega_{\rm X} = 881.8\,{\rm eV}$ is above the K edge but still close to it such that ionization by x rays is very efficient [41]. The rate of destruction of neutral and core-ionized neon by the NIR laser and the x rays is determined as follows. For photoionization by x rays, we use the total valence cross section (Ne $2s$ and Ne $2p$) at $\omega_{\rm X}$ which is $\sigma_0 = 2.3 \times 10^{-20}\,{\rm cm^2}$ for the neutral atom and $\sigma_{\vec{k}} = 3.1 \times 10^{-20}\,{\rm cm^2}$ for the core-excited cation obtained with Refs. 42 and 43. For the NIR laser, destruction by tunnel ionization occurs with the instantaneous rate $\Gamma_{0,{\rm L}}(t)$ that is determined by the ADK formula [44, 45] and the valence IP of neon 21.5645 eV [46]; at the chosen peak intensity [caption of Fig. 3], the cycle-averaged destruction rate is 0.009 eV. The ionization rate for the cation is set to zero, i.e., $\Gamma_{\vec{k},L}(t) = 0\,{\rm eV}$, because the valence IP of core-ionized states is much larger than the valence IP of the neutral atom leading to a vanishingly small width due to the exponential dependence of the ADK rate on the IP [44, 45]. Summing up all contributions yields $\Gamma_0(t) = \sigma_0\,J_{\rm X}(t) + \Gamma_{0,{\rm L}}(t)$ and $\Gamma_{\vec{k}}(t) = \Gamma_{\rm c} + \sigma_{\vec{k}}\,J_{\rm X}(t) + \Gamma_{\vec{k},L}(t)$ where $J_{\rm X}(t)$ is the instantaneous x-ray flux.

HHG spectra from Ne $1s$ core electrons for the two SASE pulses of Fig. 2 are shown in Fig. 3b together with a conventional HHG spectrum from Ne $2p$ valence electrons in Fig. 3a to facilitate a comparison. In Fig. 3b, we see an extension of the spectrum toward higher harmonic orders as well as a significant impact of the SASE pulse shape on the spectra as was also found for x-ray boosted HHG based on core excitations [21, 22]. To gain deeper insight into the temporal evolution of the emission of HHG light from core electrons, we carry out a time-frequency analysis of the dipole moment $D(t)$ giving $\tilde{\tilde{D}}(t,\omega)$. This is done with a windowed Fourier transform using a Gaussian window with a variance of 0.1 fs. The result corresponding to the black SASE pulse of Fig. 2 is shown in Fig. 4. Comparison of this plot with the time-frequency analysis of the red SASE pulse of Fig. 2 and the investigation of a difference plot reveals that the imprinting of the SASE pulse onto the HHG emission is noticeable but the general structure is determined by the NIR laser. For the 1.5-cycle NIR field, the intensity for each cycle is different, causing the highest harmonic orders to be produced at the peak of the NIR laser pulse. Then, the single maximum of the NIR laser vector potential produces the harmonic orders larger than $640\,\omega_{\rm L}$. By filtering out harmonic orders lower than $640\,\omega_{\rm L}$, we obtain the single attosecond pulses for the two SASE pulses that we fit with

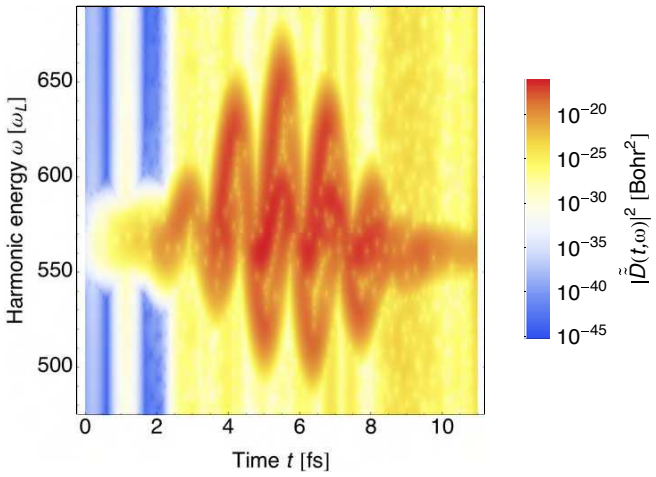

FIG. 4. (Color) Time-frequency analysis of core-electron HHG in neon for the black SASE pulses of Fig. 2.

a Gaussian profile of FWHM duration of about 160 as. The SASE pulse shape impacts only the peak intensity of the attosecond pulses.

To evaluate the efficiency of x-ray boosted HHG with Ne $1s$ core electrons, we compare it with the NIR laser-only HHG with Ne $2p$ valence electrons [Fig. 3]. Both x rays and NIR laser give rise to the same peak ionization rate. Inspecting Fig. 3, we find that the efficiency of x-ray boosted HHG is reduced by a factor of about 10^{-5} compared with the case of HHG with only the NIR laser. This can be explained by the following differences between the two HHG processes. First, the initial ionization step is mediated by either tunnel ionization or a one-x-ray-photon absorption process. Tunnel ionization occurs predominantly along the linear NIR laser polarization axis leading to a continuum electron wavepacket elongated along this axis. In contrast, one-x-ray-photon ionization of a Ne $1s$ electron produces a wavepacket with the figure-8-shape of a p_z-orbital. Hence only the part of the electron which is ejected along the NIR laser polarization axis will have a significant probability to recombine with the ionic remnant and thus contribute to HHG. Second, core-hole recombination is less efficient than valence-hole recombination. Third, valence holes are stable whereas core holes decay. Fourth, tunnel ionization releases electrons at rest but one-x-ray-photon ionization ejects electrons with a kinetic energy of $\omega_X - I_P$ [41].

Finally, we need to investigate phase matching of x-ray boosted HHG in a macroscopic medium, which is crucial for predicting the output of HHG, but becomes increasingly difficult with rising HH photon energies [27–29, 47]. From Eq. (6), we estimate the emitted photon number per pulse by $N_{\rm ph} = (n_a\,V)^2\,\Delta\Omega \int_{\omega_X}^{\infty} \frac{d^2P(\omega)}{d\omega\,d\Omega}\,d\omega$, where the atom number density is n_a and the interaction volume is $V = \pi\,w_0^2\,L$ with the NIR laser beam waist w_0, the Rayleigh range $L = \pi\,w_0^2/\lambda_L$, and the NIR laser wavelength λ_L [33]. Next $\Delta\Omega \approx 2\,\pi\,\Delta\vartheta^2$ is the solid angle of the cone of HH emission that has an opening angle ϑ along the propagation axis. We have the condition $\vartheta^2 \lesssim \lambda_L/(L\,h)$ for constructive interference in terms of the highest-generated harmonic order h. When $h = 660$, $w_0 = 30\,\lambda_L$, and $n_a = 10^{18}$ cm^{-3}, then $N_{\rm ph}$ is estimated by an order of magnitude to be about 700 which is a sufficiently high to make our boosted HHG light interesting for applications. In the attosecond pulses there are about 30 photons. Furthermore, $N_{\rm ph}$ can be increased by orders of magnitude using a higher x-ray intensity and—if one is only interested in a high HH yield—longer light pulses.

In conclusion, using x rays to ionize core electrons as a first step in HHG, we predict the high harmonics being boosted into the x-ray regime. By superimposing the harmonics close to the cutoff, we have obtained single attosecond pulses. Our scheme extends most HHG-based methods to inner-shell atomic and molecular orbitals using suitably tuned x rays.

We would like to thank Stefano M. Cavaletto, Marcelo F. Ciappina, and Markus C. Kohler for helpful discussions. C.B. was supported by the Office of Basic Energy Sciences, Office of Science, U.S. Department of Energy, under Contract No. DE-AC02-06CH11357 and by a Marie Curie International Reintegration Grant within the 7th European Community Framework Program (call identifier: FP7-PEOPLE-2010-RG, proposal No. 266551). F.H. was supported by the Pujiang scholar funding (grant No. 11PJ1404800) and the National Science Foundation of China (grant Nos. 11175120 and 11104180).

* Electronic mail; christian.buth@web.de
† Electronic mail; fhe@sjtu.edu.cn

[1] P. Agostini and L. F. DiMauro, Rep. Prog. Phys., **67**, 813 (2004).
[2] F. Krausz and M. Ivanov, Rev. Mod. Phys., **81**, 163 (2009).
[3] M. C. Kohler, T. Pfeifer, K. Z. Hatsagortsyan, and C. H. Keitel, Adv. At. Mol. Opt. Phys., in press (2012), arXiv:1201.5094.
[4] K. C. Kulander, Phys. Rev. A, **38**, 778 (1988).
[5] M. Lewenstein, P. Balcou, M. Y. Ivanov, A. L'Huillier, and P. B. Corkum, Phys. Rev. A, **49**, 2117 (1994).
[6] G. G. Paulus, W. Nicklich, H. Xu, P. Lambropoulos, and H. Walther, Phys. Rev. Lett., **72**, 2851 (1994).
[7] K. J. Schafer, B. Yang, L. F. DiMauro, and K. C. Kulander, Phys. Rev. Lett., **70**, 1599 (1993).
[8] P. B. Corkum, Phys. Rev. Lett., **71**, 1994 (1993).
[9] K. Ishikawa, Phys. Rev. Lett., **91**, 043002 (2003).
[10] S. V. Popruzhenko, D. F. Zaretsky, and W. Becker, Phys. Rev. A, **81**, 063417 (2010).
[11] E. J. Takahashi, T. Kanai, K. L. Ishikawa, Y. Nabekawa, and K. Midorikawa, Phys. Rev. Lett., **99**, 053904 (2007).

[12] K. L. Ishikawa, E. J. Takahashi, and K. Midorikawa, Phys. Rev. A, **80**, 011807 (2009).

[13] K. J. Schafer, M. B. Gaarde, A. Heinrich, J. Biegert, and U. Keller, Phys. Rev. Lett., **92**, 023003 (2004).

[14] M. B. Gaarde, K. J. Schafer, A. Heinrich, J. Biegert, and U. Keller, Phys. Rev. A, **72**, 013411 (2005).

[15] C. Figueira de Morisson Faria, P. Salières, P. Villain, and M. Lewenstein, Phys. Rev. A, **74**, 053416 (2006).

[16] A. Heinrich, W. Kornelis, M. P. Anscombe, C. P. Hauri, P. Schlup, J. Biegert, and U. Keller, J. Phys. B, **39**, S275 (2006).

[17] J. Biegert, A. Heinrich, C. P. Hauri, W. Kornelis, P. Schlup, M. P. Anscombe, M. B. Gaarde, K. J. Schafer, and U. Keller, J. Mod. Opt., **53**, 87 (2006).

[18] C. Figueira de Morisson Faria and P. Salières, Las. Phys., **17**, 390 (2007).

[19] A. Gordon, F. X. Kärtner, N. Rohringer, and R. Santra, Phys. Rev. Lett., **96**, 223902 (2006).

[20] A. Fleischer, Phys. Rev. A, **78**, 053413 (2008).

[21] C. Buth, M. C. Kohler, J. Ullrich, and C. H. Keitel, Opt. Lett., **36**, 3530 (2011), arXiv:1012.4930.

[22] M. C. Kohler, C. Müller, C. Buth, A. B. Voitkiv, K. Z. Hatsagortsyan, J. Ullrich, T. Pfeifer, and C. H. Keitel, in *Multiphoton Processes and Attosecond Physics*, Springer Proceedings in Physics (to appear in 2012) conference proceedings of the ICOMP12-ATTO3, arXiv:1111.3555.

[23] J. Arthur, P. Anfinrud, P. Audebert, K. Bane, I. Ben-Zvi, V. Bharadwaj, R. Bionta, P. Bolton, M. Borland, P. H. Bucksbaum, R. C. Cauble, J. Clendenin, M. Cornacchia, G. Decker, P. Den Hartog, S. Dierker, D. Dowell, D. Dungan, P. Emma, I. Evans, G. Faigel, R. Falcone, W. M. Fawley, M. Ferrario, A. S. Fisher, R. R. Freeman, J. Frisch, J. Galayda, J.-C. Gauthier, S. Gierman, E. Gluskin, W. Graves, J. Hajdu, J. Hastings, K. Hodgson, Z. Huang, R. Humphry, P. Ilinski, D. Imre, C. Jacobsen, C.-C. Kao, K. R. Kase, K.-J. Kim, R. Kirby, J. Kirz, L. Klaisner, P. Krejcik, K. Kulander, O. L. Landen, R. W. Lee, C. Lewis, C. Limborg, E. I. Lindau, A. Lumpkin, G. Materlik, S. Mao, J. Miao, S. Mochrie, E. Moog, S. Milton, G. Mulhollan, K. Nelson, W. R. Nelson, R. Neutze, A. Ng, D. Nguyen, H.-D. Nuhn, D. T. Palmer, J. M. Paterson, C. Pellegrini, S. Reiche, M. Renner, D. Riley, C. V. Robinson, S. H. Rokni, S. J. Rose, J. Rosenzweig, R. Ruland, G. Ruocco, D. Saenz, S. Sasaki, D. Sayre, J. Schmerge, D. Schneider, C. Schroeder, L. Serafini, F. Sette, S. Sinha, D. van der Spoel, B. Stephenson, G. Stupakov, M. Sutton, A. Szöke, R. Tatchyn, A. Toor, E. Trakhtenberg, I. Vasserman, N. Vinokurov, X. J. Wang, D. Waltz, J. S. Wark, E. Weckert, Wilson-Squire Group, H. Winick, M. Woodley, A. Wootton, M. Wulff, M. Xie, R. Yotam, L. Young, and A. Zewail, *Linac coherent light source (LCLS): Conceptual design report*, SLAC-R-593, UC-414 (2002) www-ssrl.slac.stanford.edu/lcls/cdr.

[24] P. Emma, R. Akre, J. Arthur, R. Bionta, C. Bostedt, J. Bozek, A. Brachmann, P. Bucksbaum, R. Coffee, F.-J. Decker, Y. Ding, D. Dowell, S. Edstrom, J. Fisher, A. Frisch, S. Gilevich, J. Hastings, G. Hays, P. Hering, Z. Huang, R. Iverson, H. Loos, M. Messerschmidt, A. Miahnahri, S. Moeller, H.-D. Nuhn, G. Pile, D. Ratner, J. Rzepiela, D. Schultz, T. Smith, P. Stefan, H. Tompkins, J. Turner, J. Welch, W. White, J. Wu, G. Yocky, and J. Galayda, Nature Photon., **4**, 641 (2010).

[25] V. Schmidt, *Electron spectrometry of atoms using synchrotron radiation* (Cambridge University Press, Cambridge, 1997) ISBN 0-521-55053-X.

[26] J. Tate, T. Auguste, H. G. Muller, P. Salières, P. Agostini, and L. F. DiMauro, Phys. Rev. Lett., **98**, 013901 (2007).

[27] T. Popmintchev, M.-C. Chen, A. Bahabad, M. Gerrity, P. Sidorenko, O. Cohen, I. P. Christov, M. M. Murnane, and H. C. Kapteyn, Proc. Natl. Acad. Sci. U.S.A., **106**, 10516 (2009).

[28] P. Arpin, T. Popmintchev, N. L. Wagner, A. L. Lytle, O. Cohen, H. C. Kapteyn, and M. M. Murnane, Phys. Rev. Lett., **103**, 143901 (2009).

[29] M.-C. Chen, P. Arpin, T. Popmintchev, M. Gerrity, B. Zhang, M. Seaberg, D. Popmintchev, M. M. Murnane, and H. C. Kapteyn, Phys. Rev. Lett., **105**, 173901 (2010).

[30] This description implies that the x-ray energy is quite close to the core-ionization threshold; for higher energies also destruction by double core ionization, etc. are energetically allowed.

[31] P. Meystre and M. Sargent III, *Elements of quantum optics*, 3rd ed. (Springer, Berlin, 1999) ISBN 3-540-64220-X.

[32] D. J. Diestler, Phys. Rev. A, **78**, 033814 (2008).

[33] J.-C. Diels and W. Rudolph, *Ultrashort laser pulse phenomena*, 2nd ed., Optics and Photonics Series (Academic Press, Amsterdam, 2006) ISBN 978-0-12-215493-5.

[34] I. Barth and C. Lasser, J. Phys. B, **42**, 235101 (2009).

[35] F. Herman and S. Skillman, *Atomic structure calculations* (Prentice-Hall, Englewood Cliffs, New Jersey, 1963).

[36] C. Buth and R. Santra, Phys. Rev. A, **75**, 033412 (2007), arXiv:physics/0611122.

[37] C. Buth and R. Santra, FELLA – *the free electron laser atomic, molecular, and optical physics program package*, Argonne National Laboratory, Argonne, Illinois, USA (2008), version 1.3.0, with contributions by Mark Baertschy, Kevin Christ, Chris H. Greene, Hans-Dieter Meyer, and Thomas Sommerfeld.

[38] T. Pfeifer, Y. Jiang, S. Düsterer, R. Moshammer, and J. Ullrich, Opt. Lett., **35**, 3441 (2010).

[39] Y. H. Jiang, T. Pfeifer, A. Rudenko, O. Herrwerth, L. Foucar, M. Kurka, K. U. Kühnel, M. Lezius, M. F. Kling, X. Liu, K. Ueda, S. Düsterer, R. Treusch, C. D. Schröter, R. Moshammer, and J. Ullrich, Phys. Rev. A, **82**, 041403(R) (2010).

[40] S. M. Cavaletto, C. Buth, Z. Harman, E. P. Kanter, S. H. Southworth, L. Young, and C. H. Keitel, manuscript in preparation (2012).

[41] For ω_X high above the ionization edge, the NIR laser at a chosen intensity is not strong enough to drive liberated electrons back to the atom, i.e., they cannot recombine with the parent ion and no HH light is emitted.

[42] R. D. Cowan, *The theory of atomic structure and spectra*, Los Alamos Series in Basic and Applied Sciences (University of California Press, Berkeley, 1981) ISBN 9-780-520-03821-9.

[43] Los Alamos National Laboratory, Atomic Physics Codes, http://aphysics2.lanl.gov/tempweb/lanl/.

[44] A. M. Perelomov, V. S. Popov, and V. M. Terentév, Zh. Exp. Theor. Fiz., **52**, 514 (1967), [Sov. Phys. JETP **25**, 336 (1967)].

[45] M. V. Ammosov, N. B. Delone, and V. P. Krainov, Zh. Eksp. Teor. Fiz., **91**, 2008 (1986), [Sov. Phys. JETP **64**, 1191–1194 (1986)].

[46] V. Kaufman and L. Minnhagen, J. Opt. Soc. Am., **62**,

92 (1972).

[47] M. B. Gaarde, J. L. Tate, and K. J. Schafer, J. Phys. B, **41**, 132001 (2008).